Available online at www.sciencedirect.com

SciVerse ScienceDirect

Ceramics International 38 (2012) 2537–2541

CERAMICS INTERNATIONAL

www.elsevier.com/locate/ceramint

High-temperature oxidation behavior of un-dense Ti_3AlC_2 material at 1000 °C in air

Taotao Ai

School of Materials Science and Engineering, Shaanxi University of Technology, Hanzhong 723003, China

Received 9 February 2011; received in revised form 27 October 2011; accepted 28 October 2011
Available online 15 November 2011

Abstract

Un-dense Ti_3AlC_2 material containing 3 wt% TiC was prepared by hot-pressing process using elemental powders of 2TiC/Ti/Al. Its oxidation behavior at 1000 °C in static air was investigated. SEM analysis indicates that the as fabricated sample is un-dense and the Ti_3AlC_2 grains with plate-like shape exhibit two types of fracture surfaces of layered and flat features. The oxidation behavior of the product exposed at 1000 °C for 30 h obeys a near-cubic law. The scale consists of rutile TiO_2 and α-Al_2O_3 phases, and presents three layers, including an outer un-dense TiO_2 layer adhering to a little Al_2O_3, a thick intermediate TiO_2 + Al_2O_3 mixed layer and a thin inner Al_2O_3 layer with some pores. The thickness of the oxide layer was higher than 300 μm. In addition, the deleterious effects of TiC and innate-pores on the oxidation resistance of the product were also investigated.

Keywords: A. Hot pressing; Ti_3AlC_2; Oxidation behavior; High-temperature

1. Introduction

Ti_3AlC_2 layered ternary carbide was first synthesized by Pietzka and Schuster [1] in 1994. It has unique properties of both metals and ceramics, including low density (4.25 g/cm^3), low hardness (2.0–5.0 GPa), good machinability, good chemical resistance, excellent thermal shock resistance, high strength and high Young's modulus at high temperature, as well as thermal and electrical conductivity [2–4]. Consequently, it can be used as high-temperature structural material, machinable ceramics, kiln furniture, heat exchanger, and so on. In the past decades, a variety of processes were applied and developed to synthesize Ti_3AlC_2, including hot isostatic pressing (HIP) [5], hot-pressing (HP) [6,7], self-propagating high-temperature synthesis (SHS) [8,9], spark plasma sintering (SPS) [8,10] and pulse discharge sintering (PDS) [11]. However, it is difficult to obtain high-purity Ti_3AlC_2 following a stoichiometric molar ratio of Ti:Al:C = 3:1:2, and TiC is still the main phase in the synthesized products. TiC formation by Ti–C reaction is a strong exothermal one, which could cause the abnormally expansion [11]. The high-purity Ti_3AlC_2 could be synthesized via a slightly off-stoichiometric molar ratio of Ti:Al:C = 3:1.1:1.8 [5,6]. Especially, we successfully synthesized high-purity Ti_3AlC_2 using TiC to replace graphite and a part of Ti with a molar ratio of TiC:Ti:Al = 2:1:1 [12].

As a potential high-temperature structural material, the oxidation properties of Ti_3AlC_2 in air need to be studied. Wang and Zhou [13–15] found that fully dense Ti_3AlC_2 had excellent oxidation resistance and the oxidation behavior generally obeyed parabolic law at 500–1400 °C in air. Xu et al. [16] studied the isothermal oxidation of Ti_3AlC_2 in the range of 900–1300 °C for 20 h. They found that the oxidation mechanism was controlled by the inward-diffusion of oxygen and the outward diffusion of Al when the temperature was below 1300 °C, and when above 1300 °C, it was controlled by the inward-diffusion of oxygen and the outward diffusion of Ti. Lee and Park [17] investigated the oxidation of Ti_3AlC_2 materials in air at 900–1200 °C. They displayed inconsistent oxidation behavior, due to the effect of the anisotropy of the matrix grains, the escape of carbon, the variation in the sample purity and sample density, and the variation in matrix grain size.

In this work, Ti_3AlC_2 material contained TiC was fabricated by hot pressing method using elemental powders of 2TiC/Ti/Al. The isothermal oxidation behavior of the product at 1000 °C for 30 h was studied in detail.

E-mail address: aitaotao0116@126.com.

0272-8842/$36.00
doi:10.1016/j.ceramint.2011.10.091

2. Experimental

Commercially available TiC (>99.5% purity, −200 mesh), Ti (>99.3% purity, −325 mesh) and Al (>99.5% purity, 55 μm) were used as the starting powders with a stoichiometric molar ratio of TiC:Ti:Al = 2:1:1. The mixed powders were milled for 2 h in a planetary ball mill with stainless steel containers and balls, and then pressed under 20 MPa into cylindrical specimen with a diameter of 10 mm and a height of 8 mm using isostatic pressing. The specimen was hot-pressed in vacuum at 1450 °C for 2 h. Then, the as-sintered specimen was cut into rectangular solid, and their surfaces were ground down to 1200 grit SiC sand and polished by diamond paste before oxidation experiment. The relative density of the specimen was tested by Archimedes' method.

Interrupted oxidation tests were conducted at 1000 °C in static air. The specimens were put in alumina crucibles which had been treated at a higher temperature to achieve a constant mass, then heated to the target temperature in the furnace for 1 h, and lastly taken out to cool down in ambient atmosphere as one cycle. An analytical balance with a sensitivity of 0.1 mg was used to measure the weight of the specimens at intervals during the cyclic oxidation test. The duration of the whole cyclic oxidation process was 30 cycles.

X-ray diffraction pattern (XRD, D/max 2000PC) analysis was used to identify the original composition and the oxide scales after oxidation tests. Scanning electron microcopy (SEM, JSM-6700F) equipped with energy dispersive spectrum (EDS) system was used to observe the fracture characteristic of the as-sintered product, the morphologies of the oxidized surface and the scale.

3. Results and discussion

Fig. 1 shows the XRD pattern of the as-sintered Ti_3AlC_2 product fabricated by in situ hot-pressing process at 1450 °C for 2 h. As shown in Fig. 1, the main phase is Ti_3AlC_2, and very weak TiC peaks are also identified. XRD results indicate that the high-purity Ti_3AlC_2 is not obtained. No impurities such as Fe or other compounds exist in the product because the short milling time reduces pollution. The weight percent of Ti_3AlC_2 was estimated by equations in Ref. [18], and the content of Ti_3AlC_2 is about 97%. A typical SEM micrograph of the fracture surface of the sample is shown in Fig. 2. Ti_3AlC_2 grains with plate-like shape exhibit two types of fracture surfaces of layered and flat features respectively. As can be clearly seen in Fig. 2, some lamellas are broken and pulled out, leaving many long dents which denoted by arrow. Furthermore, there are some pores in the product, and the relative density is about 95% measured by Archimedes' method.

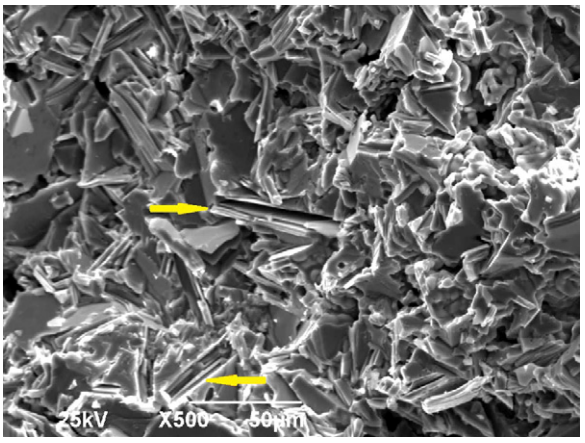

Fig. 2. SEM micrograph of the as-sintered Ti_3AlC_2 product by hot-pressing at 1450 °C for 2 h.

Fig. 3 shows the mass gain per unit area ($\Delta W/A$) of Ti_3AlC_2 product versus time (t) oxidized at 1000 °C for 30 h in air. It is found that the final mass gain per unit area is 55.54 kg/m^2, which is higher than the value in Refs. [13,14]. Obviously, the un-dense structure influences on the mass gain. Generally, if the oxidation obeys a parabolic rate law, the relations between weight gain per unit surface area ($\Delta W/A$) and the exposure time (t) can be described as follows:

$$\left(\frac{\Delta W}{A}\right)^2 = k_p t \quad (1)$$

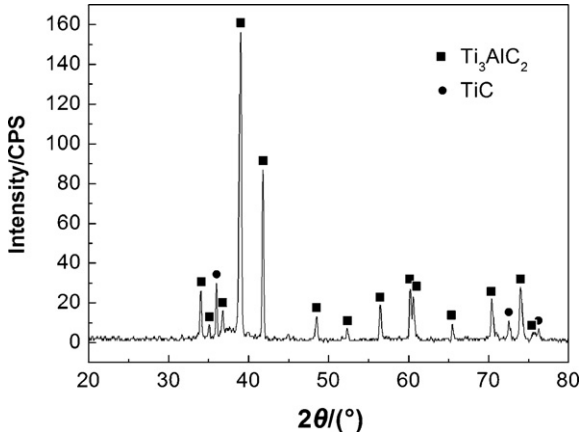

Fig. 1. X-ray diffraction pattern of the as-sintered Ti_3AlC_2 product by hot-pressing at 1450 °C for 2 h.

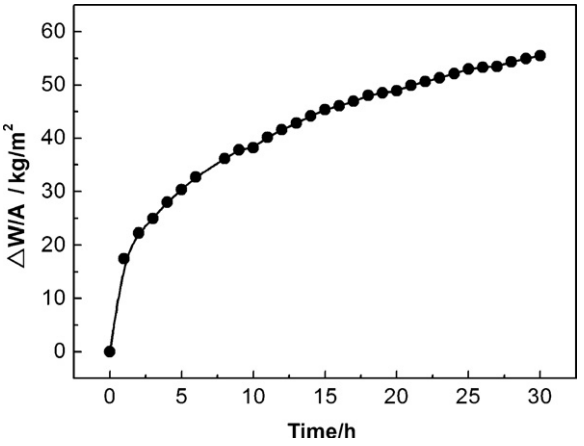

Fig. 3. Mass gain per unit area versus time for Ti_3AlC_2 oxidized in air at 1000 °C for 30 h.

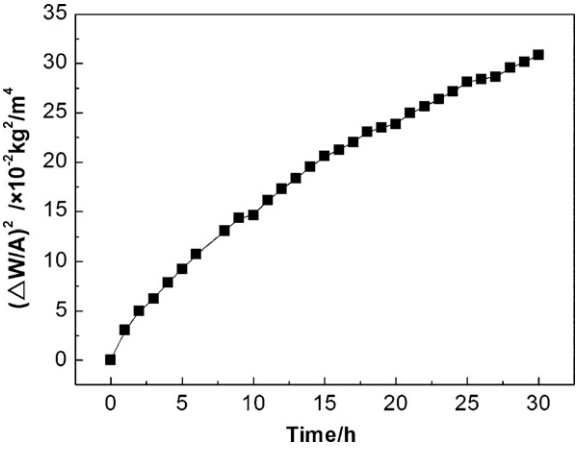

Fig. 4. Square of mass gain per unit surface area versus time for Ti_3AlC_2 oxidized in air at 1000 °C for 30 h.

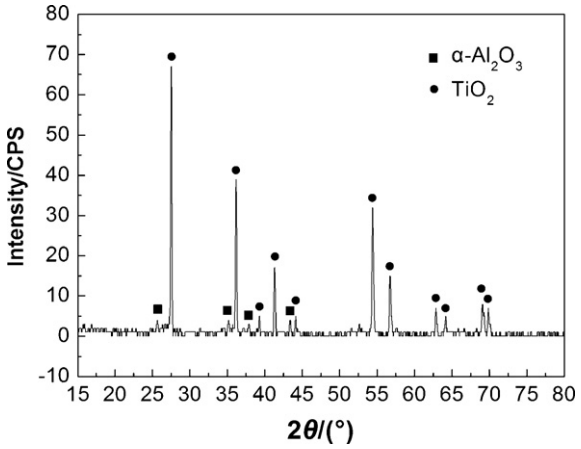

Fig. 6. X-ray diffraction pattern of the oxide scales after oxidized at 1000 °C for 30 h.

where k_p is the parabolic rate constant. Fig. 4 presents the square of mass gain per unit surface area $(\Delta W/A)^2$ versus time (t). It is obviously that the oxidation does not obey a parabolic rate law. Because the $(\Delta W/A)^2$ versus t plot shows a negative deviation from a straight line. To clarify the oxidation behavior, we attempt to fit the dates to a cubic rate law. The mass gain versus time can be described as follows:

$$\left(\frac{\Delta W}{A}\right)^3 = k_c t \tag{2}$$

where k_c is the cubic rate constant. Fig. 5 presents the cube of mass gain per unit surface area $(\Delta W/A)^3$ versus time (t). As can be seen clearly in Fig. 5, the oxidation kinetics obeys a near-cubic rate law.

Fig. 6 shows XRD pattern tested on the surface of the sample after oxidized at 1000 °C for 30 h. As shown in Fig. 6, rutile TiO_2 and α-Al_2O_3 are identified, no peaks of Ti_3AlC_2 or TiC can be observed. It indicates that the oxide scale on the surface of the product is too thick and the Ti_3AlC_2 matrix is covered with the scale, which is in accordance with the oxidation kinetics (Fig. 3).

Fig. 7 shows the SEM images of the surfaces of the sample after oxidized at 1000 °C for 30 h. The surface morphologies present an uneven feature with a lot of flutes. EDS analysis reveals that the large elongated grains in Fig. 7 are rutile TiO_2 and the small grains are Al_2O_3. The grain size of TiO_2 is much larger than that of Al_2O_3. It demonstrates that TiO_2 grows more rapidly than Al_2O_3. The isolated outward growth of large TiO_2 grains implies that the growth of TiO_2 is governed by the outward diffusion of Ti through grain boundaries of Al_2O_3. As shown in Fig. 7(b), combined with Fig. 2, it can be found that

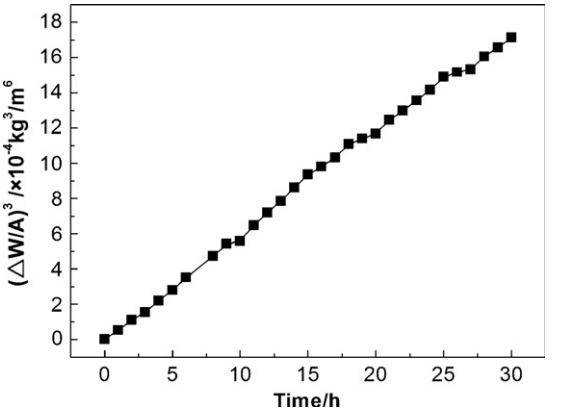

Fig. 5. Cube of mass gain per unit surface area versus time for Ti_3AlC_2 oxidized in air at 1000 °C for 30 h.

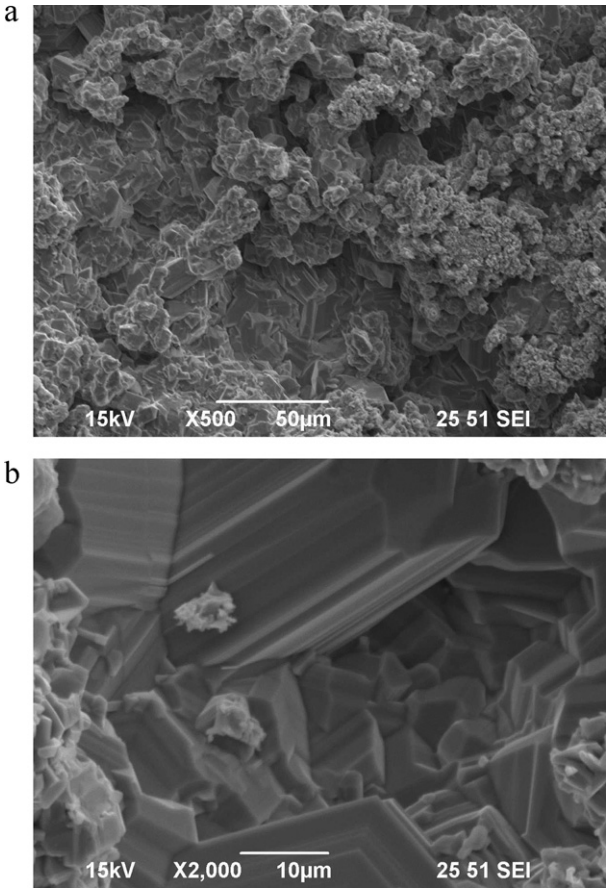

Fig. 7. Typical surface morphologies of the Ti_3AlC_2 sample after oxidized at 1000 °C for 30 h (a) low magnification and (b) high magnification.

the large elongated TiO_2 grains mostly grow along innate-pores. On the surface of these grains, there are a little Al_2O_3 grains.

Fig. 8 presents the oxide scale of the Ti_3AlC_2 sample after oxidized at 1000 °C for 30 h. The three-layer structure identified by means of EDS and the analysis of element distribution can be seen in Fig. 8, which consist of an outer un-dense TiO_2 layer adhering to a little Al_2O_3, a thick intermediate $TiO_2 + Al_2O_3$ mixed layer and a thin inner Al_2O_3 layer with some pores. From the outer layer to the inner, $TiO_2 + Al_2O_3$ mixed layer presents the transit of Ti-riched oxide to Al-riched oxide mixed layer, that having bad countercheck effects. Moreover, some pores observed in the layers will aggravate oxidizing. The total oxide-layer thickness is about 320 μm. Wang and Zhou [13] investigated the effect of TiC inclusions on the formation of protective scales by using monolithic Ti_3AlC_2 sample and Ti_3AlC_2 sample which contains TiC. It indicated that monolithic Ti_3AlC_2 had much better oxidation resistance than the Ti_3AlC_2 sample which contains TiC. In contrast to the monolithic Ti_3AlC_2 on which the flat protective scale was formed. In Figs. 7 and 8, an uneven scale is formed and a nodular structure can be observed. It indicates the outward grown TiO_2 and inward grown Al_2O_3 in the nodular area. The reason is that TiC is detrimental to the oxidation resistance and can be rapidly oxidized into TiO_2, once it is exposed to ambient atmosphere at high temperature. TiO_2 has much higher growth rate owing to its defect. When TiC/Ti_3AlC_2 material is exposed to air, the surface of TiC particles will be preferentially oxidized into TiO_2 which consequently provides fast passages for the inward diffusion of oxygen and the outward diffusion of titanium [13].

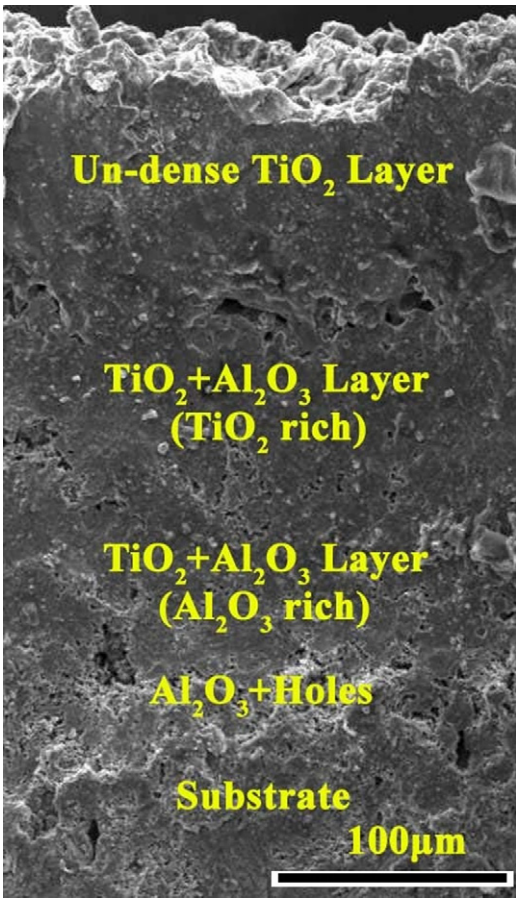

Fig. 8. Oxide scale of the Ti_3AlC_2 sample after oxidized at 1000 °C for 30 h.

Pilling et al. [19] put forward PBR theory (the volume ratio of metal atoms against oxygen atoms) in 1923. The theory considered that a protective oxide film could be formed only when PBR was a little higher than 1. For Ti/TiO_2 reaction system, the PBR value is 1.77. For Al/Al_2O_3 reaction system, the PBR value is 1.28. Thus, it can be concluded that the oxides of Ti and Al possess protection action. The reason why the mass gain is so lower in our product mainly ascribe to the un-dense structure.

With increasing of the oxidation time, the oxidation process is controlled by diffusion. At the initial stage, the diffusion medium is TiO_2. Generally, the intrinsic diffusion coefficient of oxygen or its ion in TiO_2 is too small to be determinable [20,21]. In Ref. [22], it indicated that the diffusion speed of O^{2-} in TiO_2 was independent of partial oxygen pressure, and was mostly determined by the exterior vacancy concentration created by 100–200 ppm Al_2O_3 impurity. Thus, at the preliminary stage, minute quantity of Al^{3+} dissolved in TiO_2 makes oxygen vacancy concentration rise to urge the in-diffusion of O^{2-}. Hence, the oxidizing diffusion process includes the outward diffusion of Al^{3+} and Ti^{4+}, and the inward diffusion of O^{2-}. To the end, the rapid outward diffusion of Al ion and Ti ion, and the inherent-defects results in the thick defects scale with pores, as shown clearly in Fig. 8.

In summary, the mechanism of Ti_3AlC_2 material which contains TiC oxidized at 1000 °C in air can be described as follows:

$$2Ti_3AlC_2 + 11.5O_2 \rightarrow 6TiO_2\,(\text{rutile}) + \alpha\text{-}Al_2O_3 + 4CO_2 \quad (3)$$

In the future, fully dense Ti_3AlC_2 material which contains TiC will be prepared by hot-pressing process via increasing the molding pressure. Then, the presence of TiC can be beneficial to improve the mechanical properties including hardness. The material having a higher hardness and denser structure than monolithic Ti_3AlC_2 can be applied in erosion resistant field.

4. Conclusions

Ti_3AlC_2 material which contains TiC is successfully fabricated by hot pressing method using elemental powders of 2TiC/Ti/Al. The isothermal oxidation behavior of the product at 1000 °C for 30 h was studied. The main conclusions can be summarized as follows:

(1) The content of Ti_3AlC_2 is about 97%. Un-dense structure can be observed. SEM analysis indicates that Ti_3AlC_2 grains with plate-like shape exhibit two types of fracture surfaces which are layered and flat features respectively. There are some pores in the product. The relative density of the product is about 95%.
(2) The oxidation behavior of the product after oxidized at 1000 °C for 30 h follows a near-cubic law. The final mass

gain per unit area is 55.54 kg/m^2. This phenomenon indicates that a porous material would oxidize more than a dense material as there is more surface area. The scale consists of rutile TiO_2 and α-Al_2O_3 phases, and presents an outer un-dense TiO_2 layer adhering to a little Al_2O_3, a thick intermediate $TiO_2 + Al_2O_3$ mixed layer and a thin inner Al_2O_3 layer with some pores. The thickness of oxide layer is about 320 μm. The rapid outward diffusion of Al ion and Ti ion, and the inherent-defects results in the thick defects scale with pores. The existence of TiC particles and the innate-pores are detrimental to the oxidation resistance.

Acknowledgements

We acknowledge the financial support from the Special Program of Education Bureau of Shaanxi Province of China under grant no. 2010JK467 and the Natural Science Foundation of Shaanxi Province under grant no. 2008E120.

References

[1] M.A. Pietzka, J.C. Schuster, Summary of constitutional data on the aluminum–carbon–titanium system, J. Phase Equilib. 15 (1994) 392–400.
[2] W.K. Pang, I.M. Low, B.H. O'Connor, Z.M. Sun, K.E. Prince, Oxidation characteristics of Ti_3AlC_2 over the temperature range 500–900 °C, Mater. Chem. Phys. 117 (2009) 384–389.
[3] J. Zhang, J.Y. Wang, Y.C. Zhou, Structure stability of Ti_3AlC_2 in Cu and microstructure evolution of Cu–Ti_3AlC_2 composites, Acta Mater. 55 (2007) 4381–4390.
[4] Y.C. Zhou, J.X. Chen, J.Y. Wang, Strengthening of Ti_3AlC_2 by incorporation of Si to form $Ti_3Al_{1-x}Si_xC_2$ solid solutions, Acta Mater. 54 (2006) 1317–1322.
[5] N.V. Tzenov, M.W. Barsoum, Synthesis and characterization of Ti_3AlC_2, J. Am. Ceram. Soc. 83 (2000) 825–832.
[6] X.H. Wang, Y.C. Zhou, Solid–liquid reaction synthesis of layered machinable Ti_3AlC_2 ceramic, J. Mater. Chem. 12 (2002) 455–460.
[7] J.Q. Zhu, B.C. Mei, J. Liu, X.W. Xu, Synthesis of single-phase polycrystalline Ti_3SiC_2 and Ti_3AlC_2 by hot pressing with the assistance of metallic Al or Si, Mater. Lett. 58 (2004) 588–592.
[8] A.G. Zhou, C.A. Wang, Y. Huang, Synthesis and mechanical properties of Ti_3AlC_2 by spark plasma sintering, J. Mater. Sci. 38 (2003) 3111–3115.
[9] Y. Khoptiar, I. Gotman, E.Y. Gutmanas, Pressure-assisted combustion synthesis of dense layered Ti_3AlC_2 and its mechanical properties, J. Am. Ceram. Soc. 88 (2005) 28–33.
[10] W.B. Zhou, B.C. Mei, J.Q. Zhu, X.L. Hong, Synthesis of high-purity Ti_3SiC_2 and Ti_3AlC_2 by spark plasma sintering (SPS) technique, J. Mater. Sci. 40 (2005) 2099–2100.
[11] Y. Zou, Z.M. Sun, H. Hashimoto, S. Tada, Low temperature synthesis of single-phase Ti_3AlC_2 through reaction sintering Ti/Al/C powders, Mater. Sci. Eng. A 473 (2008) 90–95.
[12] T.-T. Ai, X.-M. Feng, N.-S. Xie, F. Xu, Z. Zhao, W.H. Li, Synthesis of Ti_3AlC_2 ceramics by in-situ hot-pressing TiC/Ti/Al powders, J. Ceram. 31 (2010) 422–425 (in Chinese).
[13] X.H. Wang, Y.C. Zhou, Oxidation behavior of TiC-containing Ti_3AlC_2 based material at 500–900 °C in air, Mater. Res. Innovations 7 (2003) 381–390.
[14] X.H. Wang, Y.C. Zhou, Oxidation behavior of Ti_3AlC_2 at 1000–1400 °C in air, Corros. Sci. 45 (2003) 891–907.
[15] X.H. Wang, Y.C. Zhou, Oxidation behavior of Ti_3AlC_2 powders in flowing air, J. Mater. Chem. 12 (2002) 2781–2785.
[16] X.W. Xu, Y.X. Li, J.Q. Zhu, B.C. Mei, High-temperature oxidation behavior of $Ti_3A1\ C_2$ in air, Trans. Nonferr Metall. Soc. China 16 (2006) s869–s873.
[17] D.B. Lee, S.W. Park, High-temperature oxidation of Ti_3AlC_2 between 1173 and 1473 K in air, Mater. Sci. Eng. A 434 (2006) 147–154.
[18] C.A. Wang, A.G. Zhou, L. Qi, Y. Huang, Quantitative phase analysis in the Ti–Al–C ternary system by X-ray diffraction, Powder Diffr. 20 (2005) 218–223.
[19] Y.G. Zhang, Y.F. Han, G.L. Chen, J.T. Guo, X.J. Wan, D. Feng, Structural Intermetallics, National Defence Industry Press, Beijing, 2001 (in Chinese).
[20] J.A. Ikeda, Y.M. Chiang, Space charge segregation at grain boundaries in titanium dioxide: I. Relationship between lattice defect chemistry and space potential, J. Am. Ceram. Soc. 76 (1993) 2437–2446.
[21] J.A. Ikeda, Y.M. Chiang, Space charge segregation at grain boundaries in titanium dioxide: II. Model experiments, J. Am. Ceram. Soc. 76 (1993) 2447–2454.
[22] R. Haul, G. Dumbgen, Sauerstoff-selbstdiffusion in rutilkristallen, J. Phys. Chem. Solids 26 (1965) 1–10.